Overlap-Save FBMC receivers for massive MIMO systems under channel impairments

Fatima Hamdar, Jeremy Nadal, Charbel Abdel Nour, Amer Baghdadi

Overlap-Save FBMC receivers for massive MIMO systems under channel impairments

Fatima Hamdar[1], Jeremy Nadal[2], Charbel Abdel Nour[1], and Amer Baghdadi[1]

[1]IMT Atlantique, Lab-STICC, UMR CNRS 6285, F-29238 Brest, France
[2]Department of Electrical Engineering, Polytechnique Montreal, QC H3T 1J4, Canada

***Abstract*—Massive MIMO and filtered multi-carrier waveforms are considered as key enabling technologies for next-generation wireless networks. In this work, the Filter Bank Multi-Carrier (FBMC) waveform solution applying our previously proposed short filter and advanced receivers is extended to massive MIMO systems and evaluated in comparison to OFDM. Simulation results are presented for the non-line of sight (NLOS) 3D Urban-Macrocell (UMa) model of the 5G QuaDRiGa channel. Results show that the solution applying the proposed Overlap-Save (OS) and Overlap-Save-Block FBMC (OSB) receivers outperforms OFDM under timing offsets, carrier frequency offsets and Doppler spreads. Moreover, they confirm that the Overlap-Save FBMC receiver can support asynchronous communications in the context of massive MIMO, a cornerstone for grant-free communications and massive access.**

***Index Terms*— *Beyond 5G, massive MIMO, filtered multi-carrier waveforms, FBMC/OQAM, Overlap-Save based FBMC receivers, OFDM, time/frequency offsets, QuaDRiGa channel*.**

I. Introduction

The sixth generation (6G) of cellular networks is expected to offer higher spectral and energy efficiencies with a reduced latency, achieving an improved quality of service (QoS) compared to the fifth generation (5G) [1]. Fully exploiting large-scale multiple-input multiple-output (MIMO) systems where the base station (BS) is equipped with a large number of antennas and serves several users simultaneously represents one of the promising solutions to address part of these requirements [2], [3]. Indeed, massive MIMO (mMIMO) is already considered as one of the main technologies for 5G networks since multi-user interference can be rendered relatively negligible by increasing the number of BS antennas [4].

Due to its simplicity, robustness to multipath channels and adoption in multiple standards, OFDM was first associated with mMIMO [4] in the context of 5G and beyond systems. Despite the aforementioned advantages, it is well known that OFDM is highly sensitive to carrier frequency offsets (CFOs) as the latter leads to Inter-Carrier Interference (ICI) [5]. Furthermore, the receiver needs to be finely synchronized in time to avoid timing offset (TO) impairments. However, in order to have an energy-efficient network, the signalling overhead introduced by the synchronization procedure must be minimized. In fact, there are two scenarios to consider. The first is the relaxed synchronization scenario, in which users transmit data simultaneously. However, because each user is located at a different geographical distance from the BS, the corresponding signal is affected by a distinct propagation delay. The receiver must be able to compensate for the introduced timing offset in order to reduce energy consumption. The second scenario is the asynchronous communication scenario, in which users transmit at an independent time reference. There is no time synchronization among the scheduled users. Hence, the time mismatch between users can be as large as 50% of the symbol duration.

However, in multi-user (MU)-mMIMO systems, expected performance gains can be largely hindered by frequency and time synchronization errors between the users. Moreover, both the multi-user CFO estimation and compensation problems [6] are quite different from those in conventional single-user communication systems [7]. Therefore, preserving orthogonality across subcarriers generally requires resorting to computationally expensive techniques for mMIMO that may penalize beyond 5G system requirements in terms of throughput, energy efficiency, and latency [8]. Moreover, the orthogonality of preamble training sequences can be largely affected by TOs and/or CFOs for OFDM systems, and hence penalizing the performance [9]. Hence, taking into account the aforementioned shortcomings of OFDM, the promising benefits of MU-mMIMO systems and the stringent requirements of beyond 5G systems, there has been a regain of interest in alternative waveforms designed to address OFDM drawbacks in order to fully benefit from mMIMO technologies.

FBMC/OQAM is one of the alternative waveforms that has been investigated in recent years as an alternative to OFDM in the context of 5G. In recent years, several innovative contributions have been proposed for FBMC/OQAM in Single-Input-Single-Output (SISO) systems [10], [11]. At the transmitter side, a novel short Prototype Filter (PF) denoted by Near Perfect Reconstruction 1 (NPR1) having the same duration as one OFDM symbol was proposed to significantly reduce latency, hardware complexity and energy consumption [10]. At the receiver side, a novel FBMC receiver technique suitable for short filters was proposed [11]. The main idea was to combine a time-domain equalizer based on an Overlap-Save (OS) algorithm (for fast convolution operation) with the FBMC demodulation. The resulting receiver largely improves the robustness against double dispersive channels for short filters and enables the support of asynchronous communications. The extension of these proposals and their advantages to MU-mMIMO is not straightforward and therefore is tackled in this work. The specific contributions presented in this paper can be summarized as follows:

1) Proposal of an OS-based FBMC receivers for MU-mMIMO systems.
2) Evaluation of the performance of the OS-based FBMC receivers with the NPR1 short PF using bit error rate (BER) simulations over 5G multi-path channel under the 3D-UMA-NLOS scenario in the context of mMIMO. The results are compared to that of a typical OFDM receiver.
3) Investigation of the robustness of the different receivers to time offset impairments.

4) Study of the robustness of the different receivers to Doppler-induced frequency offset impairments.

The rest of the paper is organized as follows. In Section II, we go through relevant existing FBMC and OFDM transceivers in the context of mMIMO. The proposed OS-based FBMC receivers for MU-mMIMO are detailed in Section III. The channel model is first described in Section IV along with the used simulation tool and antenna array structure. This is followed by performance comparisons of the proposed OS-based FBMC receivers to the traditional OFDM receiver under realistic channel impairments including Doppler effect and synchronization errors. Section V concludes the paper.

II. Relevant multi-carrier transceivers in the context of massive MIMO

A. OFDM transceiver

OFDM is the predominant modulation technique used in the mMIMO literature. The OFDM transmitter is implemented using an Inverse Fast Fourier Transform (IFFT) of size M [12]. A subset of M subcarriers is chosen to carry Quadrature Amplitude Modulation (QAM) symbols for transmission. A time domain signal composed of M samples is obtained at the output of the IFFT. Finally, a cyclic prefix (CP) of length L_{CP} is inserted before the initial samples by replicating the obtained time domain signal's final L_{CP} samples. To demodulate the received signal and reconstruct the transmitted QAM symbols, the OFDM receiver applies dual operations to the ones performed by the transmitter. Due to the increased dimension of large-scale MIMO systems, a low-complexity signal detection algorithm is required. Low-complexity linear detection algorithms such as Zero Forcing (ZF) perform near-optimally if the number of antennas at the base station tends to infinity [13]. Indeed, with r being the received signal on antenna index j, which is a combination of all the signals coming from different users consisting of several OFDM symbols, an FFT of size M is required to demodulate one OFDM symbol after eliminating the CP, followed by a ZF equalization stage to separate the signals received from all users, with the equalizer matrix defined as the pseudo inverse operator $(.)^+$ of the Channel Frequency Response (CFR) $\boldsymbol{C_n}(m) = \boldsymbol{H_n^+}(m)$ for the received symbol n at frequency bin m.

B. FBMC transceiver

There are two main possible implementations for the FBMC modulation: *polyphase* network (PPN)-based [14] and *Frequency Spread* (FS)-based [15]. The first is composed of one size-M IFFT similarly to OFDM, followed by one PPN for the filtering stage. The PPN processing depends on the length of the prototype filter which is related the overlapping factor K. Using a short prototype filter (PF) (i.e $K = 1$) reduces significantly the computational complexity and latency. The offset QAM (OQAM) modulation scheme is used to preserve the orthogonality in the real field. Therefore, the PPN output signal is delayed by $M/2$ samples, and then summed with the generated signal at the previous iteration (overlapping).

Therefore, if M is the total number of subcarriers and $\boldsymbol{a_n}(m) \in \mathbb{C}^{U\times 1}$ are the users' Pulse-Amplitude Modulated (PAM) symbols at time slot n, subcarrier index m, then the baseband signal $\boldsymbol{s}(k)$ is expressed as

$$\boldsymbol{s}(k) = \sum_{n=-\infty}^{+\infty} g\left(k - n\frac{M}{2}\right)\boldsymbol{x_n}(k) \tag{1}$$

with

$$\boldsymbol{x_n}(k) = \sum_{m=0}^{M-1} (-1)^{nm}\boldsymbol{a_n}(m)\phi_n(m)e^{i2\pi\frac{km}{M}} \tag{2}$$

where $\phi_n(m) = i^{n+m}$ to keep the orthogonality in the real field.

The use of FBMC in mMIMO systems was investigated in [16], with results obtained for a sample set of channel responses generated using the IEEE802.16 broadband channel model (SUI-4) [17]. Its so-called self-equalization property, which results in a channel flattening effect, was revealed through simulations. In SISO transmissions, by using a large number of subcarriers, FBMC takes advantage of the fact that while each subcarrier band is narrow, it has an approximately flat gain and so suffers from a negligible level of Inter-Symbol Interference (ISI). However, in mMIMO systems, channel distortion is smoothed. As a result, the requirement of adopting a large number of subcarriers in FBMC systems is relaxed. This results in a lower complexity and latency caused by the analysis and synthesis filter banks. Moreover its sensitivity to CFO decreases due to the increase in subcarrier spacing. In [18] the authors propose a simple FBMC prototype filter design intended to eliminate antenna array correlation, allowing the system to reach arbitrarily high Signal to Interference Ratio (SIR) values when increasing the number of BS antennas. The authors have also shown that there is a small difference (around 1.5 dB) between the SIR of CP-OFDM and PPN-FBMC with their proposed modified prototype filter. However, they simply considered a normalized exponentially decaying channel in their simulations. Therefore, the SIR difference may get higher for more realistic channels. In [19], the PPN-FBMC low complexity data detector was implemented at the receiver side preceded by a frequency domain equalization for the received FBMC symbols. However, it was shown that the FBMC waveform with this receiver is outperformed by OFDM in the context of large-scale MIMO systems over the WINNER-Phase2 channel model due to the PPN structure of the receiver. The prior-art on FBMC-based mMIMO being still in its early stages, these systems require careful examination and investigation for being able to draw definitive conclusions.

III. Proposed OS-based FBMC receivers in the context of massive MIMO

The OS FBMC receiver was proposed for SISO transmissions in [11]. The basic principle of the OS-FBMC receiver is to integrate an OS-based time-domain equalizer with FBMC demodulation. Associated with the NPR1 short PF, this receiver was shown to achieve improved robustness against timing offsets and multipath channels with long delay spreads while reducing the computational complexity in comparison to existing FBMC receivers found in the literature [11]. Actually, there is a lot of interest in using short PF with FBMC as it enables the support of short frame sizes for low latency communication. This can significantly reduce the computational complexity, and higher power efficiency can be obtained when compared to long

PFs. Thus, implementing the OS-based FBMC receivers in the context of mMIMO becomes particularly interesting. To the best of our knowledge, this is the first time that the OS-based FBMC receivers are associated to mMIMO.

A. Overlap-Save FBMC receiver with massive MIMO

Figure 1 depicts the OS-FBMC receiver in the context of mMIMO. Let N_{Rx} be the number of antennas deployed at the receiver side, and U be the total number of users. At the output m of the size N FFT, the received signal $R_{n,m}(j)$ at receiver antenna j, symbol index n, is expressed as

$$R_{n,m}(j) = \sum_{k=0}^{N-1} r_j \left(k + n\frac{M}{2}\right) e^{-i\frac{2\pi km}{N}} \tag{3}$$

To ease notations, the received signal of all antennas can be combined into a vector $\boldsymbol{R_n}(m) = [R_{n,m}(1), ..., R_{n,m}(N_{Rx})]$. Note that $\boldsymbol{R_n}(m)$ is a combination of all the signals coming from different users consisting of several FBMC symbols. As for OFDM, MIMO equalization is performed directly after FFT as $\boldsymbol{X_n}(m) = \boldsymbol{C_n}(m) \times \boldsymbol{R_n}(m)$, where $\boldsymbol{X_n}(m)$ is the equalized signal for all users, and $\boldsymbol{C_n}(m) \in \mathbb{C}^{U \times N_{Rx}}$ is the zero-forcing equalizer matrix at frequency bin m defined in Section II-A.

Then, N_{UF} stages of circular convolution by the frequency shifted responses of the PF is performed on $\boldsymbol{X_n}(m)$, where N_{UF} is an integer number referred to as the up-sampling factor used for the OS technique. Thus, the output of each filtering stage vector is

$$\boldsymbol{Y_n}(m, \ell) = \sum_{p=-\Delta}^{\Delta} G_\ell(p) \boldsymbol{X_n}\Big(\ell + (m-p)N_{UF}\Big) \tag{4}$$

where $\Delta = (N_G - 1)/2$, N_G denotes the number of non-truncated filter coefficients, and G is the frequency shifted response of the PF that can be deduced from its impulse response g as follows

$$G_\ell(p) = e^{i\frac{\pi\ell}{N_{UF}}} \sum_{k=0}^{L-1} g(k) e^{i\frac{2\pi l(k-L/2)}{N}} e^{-i\frac{2\pi pk}{L}} \tag{5}$$

The AFB output $\boldsymbol{Y_n}(m)$, $m \in [\![0, M-1]\!]$, is obtained by summing each filtering stage vector outputs as follows

$$\boldsymbol{Y_n}(m) = \sum_{l=0}^{N_{UF}-1} \boldsymbol{Y_n}(m, \ell) \tag{6}$$

Finally, the transmitted data symbols $\hat{\boldsymbol{a}}_{\boldsymbol{n}}$(m) of all users are recovered after extracting the real part of the down-sampled (by K; K = 1 for short filters) and linear phase rotated ϕ_n filtering stage outputs

$$\hat{\boldsymbol{a}}_{\boldsymbol{n}}(m) = \mathrm{Re}\Big(\boldsymbol{Y_n}(Km)\phi_n^*(m)\Big) \tag{7}$$

B. Overlap-Save-Block FBMC receiver with massive MIMO

The OSB-FBMC receiver can be seen as an OS-FBMC receiver where the FFT is applied on a block of FBMC symbols. Hence, only one FFT is required to process all symbols in a given block. Furthermore, in the particular scenario of low mobility, it can be sufficiently accurate to assume that the channel response remains static over a given block, which reduces the equalization complexity. This is particularly interesting in mMIMO systems, as the equalization step is quite complex. Indeed, through similar demodulation steps to OS-FBMC, at the output m of the size N FFT, the received signal $R_{n,m,b}(j)$ at receiver antenna j, symbol index n in a block b, is expressed as

$$R_{n,m,b}(j) = \sum_{k=0}^{N-1} r_{b,j} \left(k + n\frac{M}{2}\right) e^{-i\frac{2\pi km}{N}} \tag{8}$$

Similarly, the equalized signal for all users $\boldsymbol{X_{n,b}}(m)$ is

$$\boldsymbol{X_{n,b}}(m) = \boldsymbol{C_{n,b}}(m) \times \boldsymbol{R_{n,b}}(m) \tag{9}$$

where $\boldsymbol{C_{n,b}}(m) \in \mathbb{C}^{U \times N_{Rx}}$ is $\boldsymbol{C_n}(m)$ for a block b, and $\boldsymbol{R_{n,b}}(m) = [R_{n,m,b}(1), ..., R_{n,m,b}(N_{Rx})]$ is a combination of all the signals coming from different users consisting of several blocks of FBMC symbols.

Hence, if $\hat{\boldsymbol{a}}_{\boldsymbol{n,b}}$(m) is the recovered PAM symbol at block b and FBMC symbol n for all users, we have:

$$\hat{\boldsymbol{a}}_{\boldsymbol{n,b}}(m) = \mathrm{Re}\Big(\boldsymbol{Y_{n,b}}(Km)\phi_n^*(m)\Big) \tag{10}$$

where $\boldsymbol{Y_{n,b}}(m)$ is the AFB output expressed as

$$\boldsymbol{Y_{n,b}}(m) = \sum_{l=0}^{\mathrm{N}_{UF}-1} \sum_{p=-\Delta}^{\Delta} G_\ell(p) \boldsymbol{X_{n,b}}(Km-p, l) \tag{11}$$

and N_{UF} is chosen so that it is the lowest possible integer value considering that the FFT size must be superior or equal to the block size N_s:

$$N_{UF} = \left\lceil 1 + \frac{N_s - 1}{2K} \right\rceil \tag{12}$$

IV. Simulation Results

In this section, we first describe the used filtered discrete channel model, the simulation tool and the antenna array structure. Then, the performance of the OS-FBMC and OSB-FBMC receivers, using the NPR1 short PF, is evaluated in the context of mMIMO. Several channel impairments are considered such as timing offsets, Doppler effect, and carrier frequency offsets. The results are then compared to the OFDM waveform with 4 and 16-QAM. In our simulations, the Channel State Information (CSI) is assumed to be perfectly known at the receiver side. Furthermore, the number of non-truncated filter coefficients is set to $N_G = 7$ for an SIR of 55 dB [10]. For the OS-FBMC based receivers, the up-sampling factor used for the OS technique is set to $N_{UF} = 4$ which is a good compromise between system performance and complexity. The number of FBMC symbols in a block N_s for the OSB-FBMC receiver is set to 7. This is reflected by the OS_4-FBMC and OSB_7-FBMC receiver notations.

A. Simulation setup

1) Channel model: In rapidly changing environments, a discrete multipath channel model has, in general, a variable number of paths in addition to variable path gains. However, for reference channels it can be assumed that the number of discrete components is constant. Consider a channel model consisting of

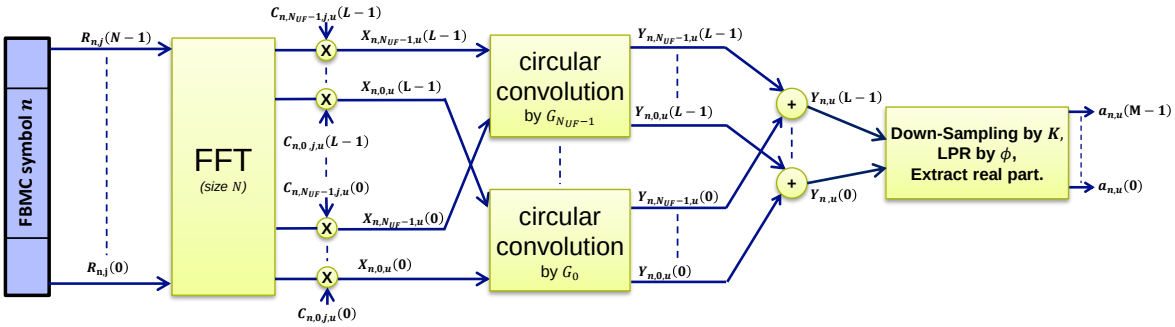

Fig. 1. OS-FBMC/OQAM massive MIMO Receiver.

M' paths, then for antenna k, and user u, the channel impulse response $h_u(k,t)$ is given by

$$h_u(k,t) = \sum_{m=1}^{M'} b_{m,u}(k)\delta(t - \tau_{m,u}(k)) \tag{13}$$

where M' is the total number of paths, k is the antenna index, m is the path index, u is the user index, $\tau_{m,u}(k)$ is the path delay, and $b_{m,u}(k)$ is the path complex amplitude.

According to [20], when the differential delays are small compared to the simulation sampling time T_s or are not integer multiples of T_s, it is advantageous to band limit the channel by design to obtain better simulation properties. Hence, the channel impulse response is band-limited using an ideal rectangular filter. Thus, the filtered discrete channel impulse response is given by

$$\tilde{h}(k,n) = \sum_{m=1}^{M'} b_{m,u}(k) sinc(\frac{\tau_{m,u}(k)}{T_s} - n), -N_1 \leqslant n \leqslant N_2 \tag{14}$$

where N_1 and N_2 are the tap indices chosen so that $\tilde{h}(k,n)$ is small when n is less than N_1 or greater than N_2, and $sinc(x) = sin(x)/x$ [21]. In our simulations, the tap indices are chosen so that the value of $\tilde{h}(k,n)$ at the relevant tap indices is greater by at least 1% of its maximum.

According to [22], if the maximum distance between antenna elements divided by the speed of light $(d_{\max}/c)$ is much smaller than $\frac{1}{B}$ value, where B is the transmission bandwidth, the delay value can be assumed independent of antenna index k, i.e. $\tau_{m,u}(k) = \tau_{m,u}$.

2) Simulation tool: QuaDRiGa (QUAsi Deterministic RadIo channel GenerAtor) [23] was developed to enable the modeling of MIMO radio channels for specific network configurations, such as indoor, satellite, etc. QuaDRiGa incorporates a set of characteristics developed in the Spatial Channel Model (SCM) [24] and WINNER channel models [25], as well as modeling methodologies to enable quasi-deterministic multi-link tracking of users' movements in changing environments. For our simulations QuaDRiGa is used to generate realistic radio channels. Chosen parameters follow the 5G standard [26] with cross-polarized 64 antennas at the BS.

Parameters	Value
Carrier frequency	3.5 GHz
Cyclic prefix	36
Channel model	'3GPP_3D_UMa'
Channel type	NLOS
Total number of subcarriers	512 subcarriers
Sub-band size	300 subcarriers
N of UE	4
BS height	25 m
N of BS antennas	64
N of vertical panels	2
N of Horizontal panels	1
vertical panel spacing	85.7 mm
Vertical antennas spacing	42.85 mm
Horizontal antennas spacing	42.85 mm

TABLE I
SIMULATION PARAMETERS

3) Antenna array structure: For the 3D-Uma NLOS model of the 5G Quadriga channel, the BS's antenna array is 25 meters high and consists of two co-located rectangular sub-arrays, each with 32 antennas as in [27]. Each sub-array is denoted by (N_V, N_H, N_P) as shown in Fig. 2, where N_H = 2 is the number of columns, N_V = 8 is the number of antenna elements with the same polarization in each column, and N_P = 2 is the number of polarizations as proposed in [28]. Therefore, with $N_{gV} = 2$ vertical antenna panels, the number of antennas is calculated as $N_{RX} = N_{gV}N_V N_H N_P$ = 64. With λ being the carrier wavelength, the 2 antenna panels are spaced in the vertical direction with a spacing of $d_{gV} = \lambda$, and the antenna units placed inside each panel are uniformly spaced in the horizontal direction with a spacing of $d_H = 0.5\lambda$ and in the vertical direction with a spacing of $d_V = 0.5\lambda$, where $\lambda = 85.7$ mm for a carrier frequency $f_c = 3.5$ GHz. Specific simulation parameters are specified in Table I.

B. BER performance over static channels

The BER performance of the OS-based FBMC receivers is compared to OFDM on the 5G channel with the 3D UMa-NLOS scenario. Simulation parameters are summarized in Table I. The channel is considered to be static (i.e: the users are stationary).

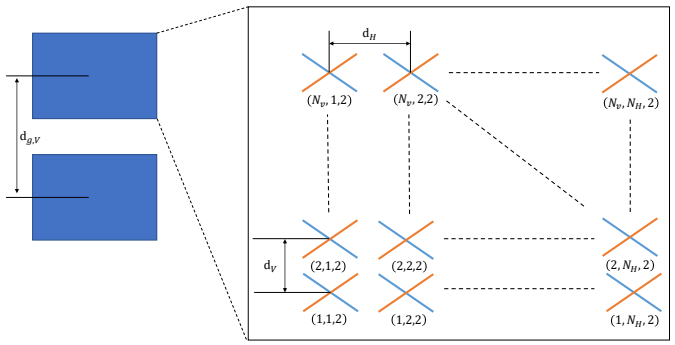

Fig. 2. Cross polarized antenna array structure

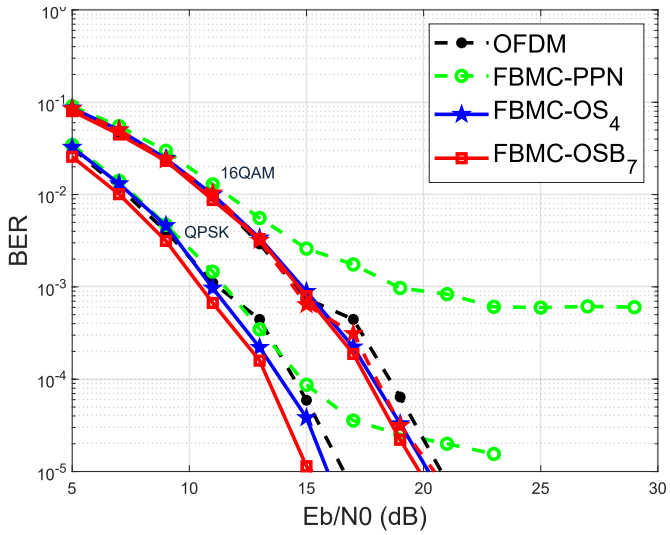

Fig. 3. BER performance comparison of considered waveforms over the 5G Quadriga fading channel under the '3GPP-3D-UMA-NLOS' scenario', with 4 users and 64 Rx antennas.

1) Multipath channel: Although one of the historic drawbacks of FBMC compared to OFDM resides in the difficulty of efficiently supporting mMIMO systems because of the lack of orthogonality in the complex plane between neighboring OQAM symbols, we can see in Figure 3 that OFDM is outperformed by the proposed FBMC waveform thanks to the OS-based FBMC receivers. Indeed, the FBMC-OSB$_7$ receiver shows the best performance. Furthermore, since the PPN-FBMC technique was widely adopted in prior-art related to mMIMO, it was taken as reference for FBMC proposals. As depicted in Figure 3, PPN-FBMC offers the worst performance, suffering from an error floor. This result is expected as it was previously demonstrated with SISO transmissions in [10].

2) Timing offsets: In the uplink, the timing advance mechanism [29] is used to compensate for the propagation delay of each user located at a different geographical distance from the BS. However to reduce power consumption in future beyond 5G systems, it is preferable to adopt a relaxed synchronization where the propagation delay of each user is not compensated, hence avoiding the timing advance mechanism. Therefore, the resulting synchronization errors would cause linear phase rotations for each subcarrier. For the FBMC waveform and proposed

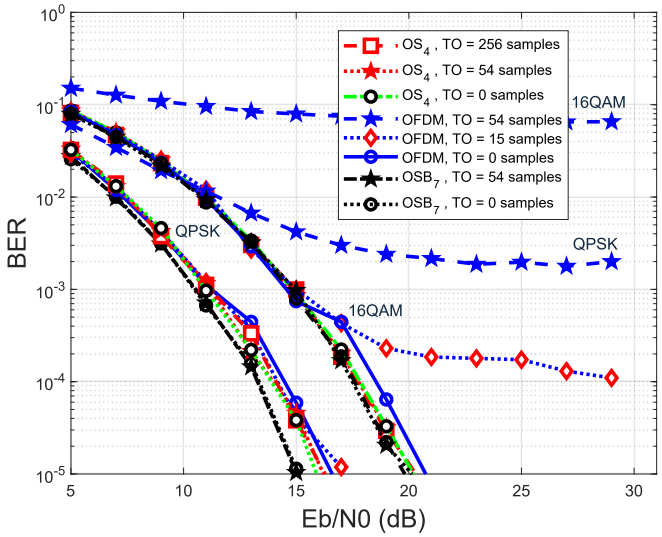

Fig. 4. BER performance comparison of different receivers in the presence of timing offset over the 5G Quadriga fading channel under the '3GPP-3D-UMA-NLOS' scenario', with 4 users and 64 Rx antennas.

receivers, these can be totally compensated after channel estimation and equalization. Therefore, if l_d is the time offset in number of samples, then the frequency domain compensation term is expressed as $C_{TO}(m) = e^{-i\frac{2\pi m l_d}{N'}}$ where $N' = M$ for OFDM, and $N' = N_{UF}M$ for the OS-based FBMC receivers. It is assumed that the timing offset l_d is perfectly known at the receiver side.

For our simulations, the receiver is considered perfectly time-aligned when the first sample processed by the FFT is the sample located at the middle of the CP length, so that both positive and negative TO values can be supported. It is well known that OFDM will be free from any interference, and orthogonality is perfectly restored if and only if the timing offset $|l_d| < \frac{L_{CP}}{2}$ where L_{CP} is the length of the cyclic prefix. Therefore, a TO of 15 samples is applied to the OFDM waveform, that corresponds to approximately 42% of L_{CP}. Figure 4 shows the BER performance of OFDM, and the OS-based FBMC receivers respectively in the presence and absence of timing offset. As depicted in the figure, with the 16QAM modulation scheme, the OFDM waveform starts to suffer from a performance degradation. This confirms that OFDM is highly sensitive to TO impairments. After that, a TO of 54 samples is applied that corresponds to 10.55% of the symbol period and is 3 times greater than the CP size. As depicted in Figure 4, the OFDM waveform suffers from severe performance degradation. Unlike OFDM, the OS-based FBMC receivers show robustness against a timing offset of 54 samples where their BER performance wasn't affected at all as shown in the same figure.

Regarding the OS$_4$-FBMC receiver, a timing offset of 256 samples (half the symbol duration) was applied, and as depicted in the same Figure 4, there is no effect observed on the BER performance, which means that the OS$_4$-FBMC receiver is able to support any timing offset value less than half the symbol duration which makes it adequate for asynchronous communication in the context of mMIMO.

Unlike the OS$_4$-FBMC receiver, the OSB$_7$-FBMC receiver

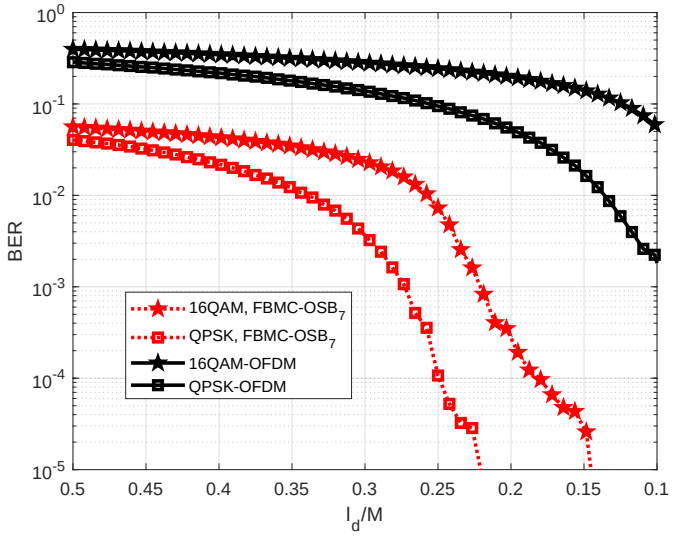

Fig. 5. Timing offset evaluation in terms of BER for the OSB$_7$-FBMC and OFDM receivers over the 5G Quadriga fading channel under the '3GPP-3D-UMA-NLOS' scenario', with 4 users and 64 Rx antennas.

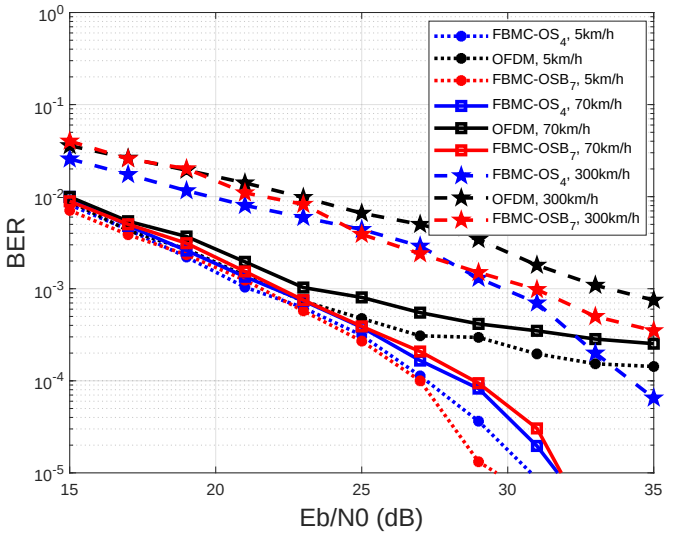

Fig. 6. BER performance for different receivers over the non-static 5G Quadriga fading channel under the '3GPP-3D-UMA-NLOS' scenario', with 4 users and 64 Rx antennas.

cannot support any timing offset value less than half the symbol duration, because, for certain timing offset value the generated interference will no longer be limited, resulting in irreducible errors. Since in the OSB-FBMC receiver, FBMC symbols are transmitted in blocks and demodulated all at once in the frequency domain, the receiver processing window must, to some extent, be aligned with the received blocks. However, because of the PF's ramp-up and down, the OSB-FBMC receiver is less susceptible to timing offset impairments than OFDM.

Actually, in order to know what is the maximum value of the timing offset such that the OSB$_7$-FBMC receiver will still able to limit interference, we plot in Figure 5 the BER performance versus l_d/M of the OSB$_7$ and OFDM receivers. For this simulation, noise is removed, corresponding to a transmission at infinite Signal-to-Noise Ratio (SNR).

As depicted in the figure, the OSB$_7$-FBMC receiver with QPSK can support a timing offset of 22% of the symbol period for an error floor less than 10^{-5}. However, with 16QAM modulation scheme, it can only support a timing offset up to 14% of the symbol period. For larger timing offset values, the error floor gradually increases showing that the interference introduced is not limited. However, it is worth noting that the OSB$_7$-FBMC receiver is more robust against timing offset than OFDM in the context of mMIMO, as it was also the case in SISO transmissions [11].

C. BER performance over non-static channel

It is well known that OFDM is very sensitive to carrier offsets caused by Doppler spread/shift [5]. In fact, the impact of Doppler spread/shift on the system performance is worse in MU-mMIMO systems as the achievable gains of mMIMO heavily depend on the accuracy of frequency synchronization.

1) Doppler spread: We consider users moving with speeds of 5, 70, and 300 km/h and test the BER performance of FBMC when using the OS-based FBMC receivers compared to OFDM on the non-static 5G channel with the UMa-NLOS scenario. The results are shown in Figure 6. The BER performance is degraded compared to that in a static channel. For a speed of 5km/h, similar BER levels are obtained for the OFDM, the OS$_4$-FBMC, the OSB$_7$-FBMC receivers when we have Eb/N0 < 25 dB. However, OFDM shows the worst BER performance when we have Eb/N0 > 25 dB. Despite the fact that the maximum Doppler shift is substantially less than the subcarrier spacing, OFDM has around a 10^{-4} error floor due to its low frequency localization. Similar observations can be made with a speed of 70 km/h, presented in the same Figure 6. OFDM once again shows the worst performance. The OS-based FBMC receivers have similar performance and outperform OFDM. For a speed of 300km/h, the performance is highly degraded for all receivers. The OSB$_7$-FBMC receiver performs worse than the OS$_4$-FBMC receiver, yet it's worth noting how it outperforms OFDM as the latter suffers from an error floor of approximately 10^{-3}. In fact, it's noteworthy how the OS$_4$-FBMC receiver offers the best performance, but it comes at the expense of system simplicity when compared to OFDM.

2) Carrier frequency offset: CFO also arises when the transmitter and receiver's local oscillators have a frequency misalignment which happens when using low-cost oscillators. Mathematically, this corresponds to a linear phase rotation of the received baseband samples. Therefore, if S is the transmitted signal, then the received signal R in the presence of CFO will be $R(k) = S(k)e^{-i\frac{2\pi kr}{M}}$, where r is the CFO relative to the subcarrier spacing (Δf). In reality, CFO causes two types of impairments at the receiver. The first one is the Common Phase Error (CPE), which may be easily compensated in the frequency domain if the CFO is estimated. The second drawback is ICI, which is caused by frequency domain misalignment of the transmitter and receiver PFs. The second drawback is a significant problem for OFDM because of its low frequency localization. However, the Frequency Domain Compensation (FDC) technique can be used to compensate the CFO for FBMC [10], resulting in a large reduction in the ICI caused by the CFO. This is a key benefit for FBMC since it relaxes the frequency synchronization requirement, allowing for higher

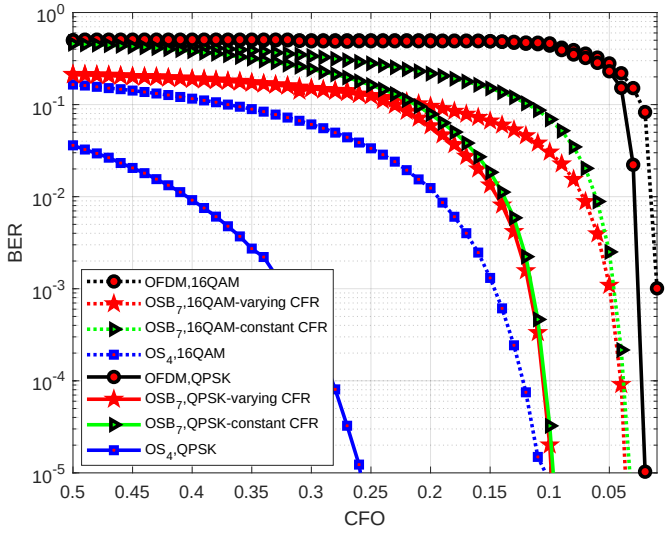

Fig. 7. Carrier frequency offset evaluation in terms of BER for different receivers with 4 users and 64 Rx antennas.

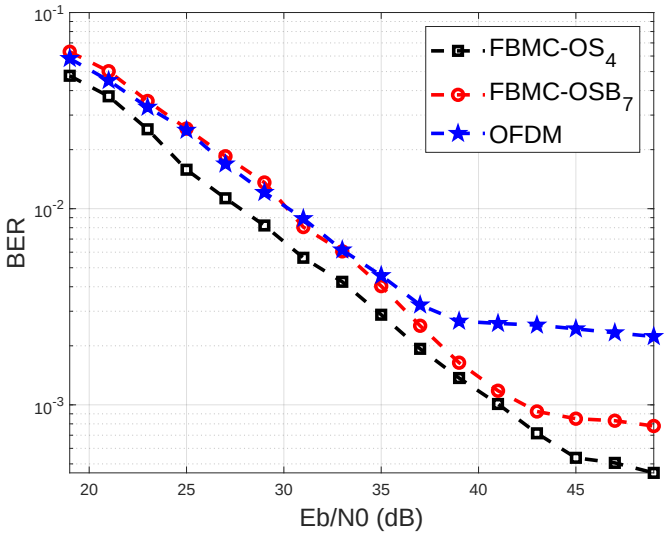

Fig. 8. BER performance comparison for all receivers over the 5G Quadriga fading channel under the '3GPP-3D-UMA-NLOS' scenario' considering P_s = 0 dBW, zero gaurdbands, with 3 users, and 64 Rx antennas.

speeds and the use of low-cost oscillators. In this regard, we study the robustness of each receiver to CFO resulting from the frequency misalignment of local oscillators. Figure 7 shows the BER performance versus CFO for all receivers without noise (infinite SNR). In this case, the CPE term to compensate is $e^{j\pi nr}$, and the CFO is assumed to be perfectly known at the receiver side. As expected, OFDM shows the worst performance. In the OSB-FBMC receiver described before, equalization is performed for each FBMC symbol n in a block b. This increases the equalization complexity compared to the OFDM signal, however, allows to accurately compensate fast varying channels. Hence, with QPSK, the OSB$_7$-FBMC receiver with varying CFR can tolerate a CFO of 10% of Δf for an error floor of around 10^{-5}, however, only 4% of Δf with the 16-QAM modulation scheme. For larger CFO values, the error floor gradually increases showing that the interference introduced is not limited. On the other hand, it is assumed that the equalizer coefficients $\boldsymbol{C_{b,n}}(m)$ in (9) are independent of n ($\boldsymbol{C_{b,n}}(m) = \boldsymbol{C_b}(m)$). This means that the channel is constant over a block b in the OSB$_7$-FBMC receiver, which reduces the equalization complexity but degrades the performance at larger CFOs as shown in the same figure. The OS$_4$-FBMC receiver offers the best performance, where it can support a CFO of 26% and 10% of Δf with the QPSK and 16QAM modulation schemes respectively for an error floor around 10^{-5}.

D. BER performance in the presence of two Interferers

It is well known that the multi-user interference vanishes in mMIMO systems due to the large antenna array at the BS. Therefore, in this subsection, we demonstrate a communication in which several users transmit data on adjacent frequency bands. However, the communication is done asynchronously in time, which means that the users do not agree on when the signals should be transmitted. As a result, signals arrive with random delays. In this scenario, We examine three transmission channels operating in parallel on 1.5 MHz bands, this means 4.5 MHz. The second transmission (middle of the band) will be considered as the "main" transmission which will be demodulated by the receiver. The other two transmissions (in the upper and lower parts of the total band) will be treated as interferers with the main transmission. The transmit powers of all transmissions are assumed to be equal and normalized to $P_s = 0$ dBW, and no guardband is used. Figure 8 compares the BER performance of all receivers under this scenario in the context of mMIMO. Due to the low frequency localization of OFDM, it is highly affected by the adjacent interferes leading to the highest error floor when compared to FBMC. However, FBMC augmented by the OS-based receivers is more robust against adjacent interferers compared to OFDM thanks to the frequency localization of the NPR1 PF. It's also worth noting that the OS$_4$-FBMC receiver offers the best performance. This is due to its support to asynchronous communication in the context of mMIMO as was demonstrated in Subsection IV-B2. In fact, we can deduce that FBMC requires less gaurdbands than OFDM. Hence, FBMC is more bandwidth-efficient.

V. Conclusion

This article extends the use of OS-based FBMC receivers with short filters to the context of MU-mMIMO and investigates their advantages in comparison to OFDM under different channel impairments. The results reveal that in the 3D-UMa NLOS scenario, the proposed FBMC transceivers outperform OFDM over the 5G static and non-static channels. The first appealing benefit of the FBMC waveform with OS-based receivers resides in its robustness against timing offsets when compared to OFDM, even enabling asynchronous communications. Moreover, simulation results confirm its superiority compared to OFDM under severe channel impairments caused by carrier frequency offsets and Doppler effects. Consequently, augmented by the OS-based receivers, the FBMC-OQAM waveform becomes a promising challenger of OFDM in the context of MU-mMIMO.

REFERENCES

1 Yang, P., Xiao, Y., Xiao, M., and Li, S., "6G Wireless Communications: Vision and Potential Techniques," *IEEE Network*, vol. 33, no. 4, pp. 70–75, 2019.

2 Swindlehurst, A. L., Ayanoglu, E., Heydari, P., and Capolino, F., "Millimeter-wave Massive MIMO: the next wireless revolution?" *IEEE Commun. Mag.*, vol. 52, no. 9, pp. 56–62, 2014.

3 Busari, S. A., Huq, K. M. S., Mumtaz, S., Dai, L., and Rodriguez, J., "Millimeter-Wave Massive MIMO Communication for Future Wireless Systems: A Survey," *IEEE Commun. Surveys Tutorials*, vol. 20, no. 2, pp. 836–869, 2018.

4 Marzetta, T. L., "Noncooperative Cellular Wireless with Unlimited Numbers of Base Station Antennas," *IEEE Trans. on Wireless Commun.*, vol. 9, no. 11, pp. 3590–3600, 2010.

5 Sathananthan, K. and Tellambura, C., "Probability of error calculation of OFDM systems with frequency offset," *IEEE Trans. on Commun.*, vol. 49, no. 11, pp. 1884–1888, 2001.

6 Sabeti, P., Farhang, A., Marchetti, N., and Doyle, L., "CFO Estimation for OFDM-Based Massive MIMO Systems in Asymptotic Regime," in *2018 IEEE 10th Sensor Array and Multichannel Signal Processing Workshop (SAM)*, 2018, pp. 99–103.

7 Schmidl, T. and Cox, D., "Robust frequency and timing synchronization for OFDM," *IEEE Trans. on Commun.*, vol. 45, no. 12, pp. 1613–1621, 1997.

8 Banelli, P., Buzzi, S., Colavolpe, G., Modenini, A., Rusek, F., and Ugolini, A., "Modulation formats and waveforms for 5g networks: Who Will Be the Heir of OFDM?: An overview of alternative modulation schemes for improved spectral efficiency," *IEEE Signal Process. Mag.*, vol. 31, no. 6, pp. 80–93, 2014.

9 Yang, F., Cai, P., Qian, H., and Luo, X., "Pilot contamination in massive mimo induced by timing and frequency errors," *IEEE Trans. on Wireless Commun.*, vol. 17, no. 7, pp. 4477–4492, 2018.

10 Nadal, J., Nour, C. A., and Baghdadi, A., "Design and Evaluation of a Novel Short Prototype Filter for FBMC/OQAM Modulation," *IEEE Access*, vol. 6, pp. 19 610–19 625, 2018.

11 Nadal, J., Leduc-Primeau, F., Nour, C. A., and Baghdadi, A., "Overlap-save FBMC Receivers," *IEEE Trans. on Wireless Commun.*, vol. 19, no. 8, pp. 5307–5320, 2020.

12 Bingham, J., "Multicarrier modulation for data transmission: an idea whose time has come," *IEEE Commun. Mag.*, vol. 28, no. 5, pp. 5–14, 1990.

13 Rusek, F., Persson, D., Lau, B. K., Larsson, E. G., Marzetta, T. L., Edfors, O., and Tufvesson, F., "Scaling Up MIMO: Opportunities and Challenges with Very Large Arrays," *IEEE Signal Process. Mag.*, vol. 30, no. 1, pp. 40–60, 2013.

14 Hirosaki, B., "An Orthogonally Multiplexed QAM System Using the Discrete Fourier Transform," *IEEE Trans. on Commun.*, vol. 29, no. 7, pp. 982–989, 1981.

15 Bellanger, M., "FS-FBMC: An alternative scheme for filter bank based multicarrier transmission," in *2012 5th Intl. Symposium on Commun., Control and Signal Process.*, 2012, pp. 1–4.

16 Farhang, A., Marchetti, N., Doyle, L. E., and Farhang-Boroujeny, B., "Filter Bank Multicarrier for Massive MIMO," in *IEEE 80th Veh. Tech. Conf. (VTC2014-Fall)*, 2014, pp. 1–7.

17 Hari, K., Baum, D., Rustako, A., Roman, R., and Trinkwon, D., "Channel models for fixed wireless applications," *IEEE 802.16 Broadband wireless access working group*, 2003.

18 Aminjavaheri, A., Farhang, A., Doyle, L. E., and Farhang-Boroujeny, B., "Prototype filter design for FBMC in massive MIMO channels," in *IEEE Intl. Conf. on Commun. (ICC)*, 2017, pp. 1–6.

19 Tunali, N. E., Wu, M., Dick, C., and Studer, C., "Linear large-scale MIMO data detection for 5G multi-carrier waveform candidates," in *49th Asilomar Conf. on Signals, Systems and Computers*, 2015, pp. 1149–1153.

20 Jeruchim, M. C., Balaban, P., and Shanmugan, K. S., *Simulation of Communication Systems, Second Edition, New York, Kluwer Academic/Plenum*, 2000.

21 https://www.mathworks.com/help/comm/ug/fading-channels.html/.

22 Osinsky, A., Ivanov, A., and Yarotsky, D., "Theoretical Performance Bound of Uplink Channel Estimation Accuracy in Massive MIMO," in *IEEE Intern. Conf. on Acoustics, Speech and Signal Proc. (ICASSP)*, Barcelona, Spain, 2020, pp. 4925–4929.

23 https://quadriga-channel-model.de/.

24 3GPP TR 25.996, v14.0.0, "Spatial channel model for multiple input multiple output (MIMO) simulations", 2017.

25 Kyösti, P., Meinilä, J., Hentilä, L., Zhao, X., Jämsä, Schneider, T., and Christian Milan Narandzić, A. H. J. Y. V.-M. H. M. A. R. B. Y. d. J. T. R., "IST-4-027756 WINNER II D1.1.2 v.1.1: WINNER II channel models," 2007. [Online]. Available: http://www.ist-winner.org

26 3GPP TR 138 901, v15.0.0, "5G; Study on channel model for frequencies from 0.5 to 100 GHz", 2018.

27 Ivanov, A., Osinsky, A., Lakontsev, D., and Yarotsky, D., "High Performance Interference Suppression in Multi-User Massive MIMO Detector," in *IEEE 91st Veh. Tech. Conf. (VTC2020-Spring)*, 2020.

28 Liu, G., Hou, X., Jin, J., Wang, and andothers, "3-D-MIMO With Massive Antennas Paves the Way to 5G Enhanced Mobile Broadband: From System Design to Field Trials," *IEEE J. on Selected Areas in Commun.*, vol. 35, no. 6, pp. 1222–1233, 2017.

29 3GPP TS 36.211,"Technical specification group radio access network; physical channels and modulation", http://www.3gpp.org/dynareport/36211.htm.